Analyst

PAPER

View Article Online
View Journal | View Issue

Cite this: *Analyst*, 2025, **150**, 2295

Spectral imaging and a one-class classifier for detecting elastane in cotton fabrics†

Ella Mahlamäki, *[a] Inge Schlapp-Hackl, [b] Tharindu Koralage, [b] Michael Hummel [b] and Mikko Mäkelä [a]

Received 28th January 2025,
Accepted 2nd April 2025

DOI: 10.1039/d5an00107b

rsc.li/analyst

Elastane detection is important for textile recycling as elastane fibers can hamper mechanical and chemical fiber recycling. Here, we report the use of near-infrared imaging spectroscopy and class modelling to detect 2–6% elastane in consumer cotton fabrics to provide alternatives to current detection methods, which are invasive and time-consuming. Our method automatically identified outlier fabrics and measurements with class-specific clustering and showed higher classification accuracies by averaging across individual pixel spectra to reduce sampling uncertainty. The final classification results showed median test set true positive and true negative rates of 89–97% based on randomized resampling. Class modelling offers clear benefits compared to commonly used discriminant classifiers as it allows modelling new classes using only a set of target samples without requiring representative training objects from all the other classes. Overall, these results open the possibility for fast non-invasive detection of small amounts of elastane in cotton, taking us a step closer to a circular economy of textiles.

1. Introduction

The discovery of polyurethanes is often credited to Otto Bayer who found that diols and diisocyanates react readily in a condensation reaction.[1] The underlying principle of hard polyurethane fibers paved the way for the development of highly elastic fibers nowadays known as elastane in continental Europe. In some other countries the names spandex and lycra have become proprietary on the market. Elastane is used in apparel to provide stretch, flexibility, and comfort to clothing items allowing for better mobility and fit, particularly in garments like sportswear and leggings that require flexibility during physical activities. Although the exact composition of elastane fibers can differ depending on the manufacturer, they all consist of polyurethanes. The resulting fibers have tenacities up to 15 cN tex^{-1} at elongation to break values of 200–800% with almost complete elastic recovery up to 500%.[2] Only small quantities of these fibers are needed in fiber blends to produce form-fitting apparel due to these outstanding properties. Apparel products thus frequently contain elastane and the share of elastane containing textiles is increasing. The global production of elastane fibers declined for the first time to 1.1 million tons in 2022 after hitting its all-time production high of 1.2 million tons in 2021.[3,4] Of these overall volumes, approximately 2.6% is estimated to be recycled elastane.[3]

We report a novel method to detect elastane in cotton fabrics based on near infrared (NIR) imaging spectroscopy and class modelling. Cotton, together with regenerated cellulosic fibers viscose and Lyocell, covers 32% of global textile fiber production,[5] and is often combined with elastane for clothing applications. The same elastane properties that provide clear benefits in clothing, however, complicate several unit operations during textile recycling. For example, end-of-life textiles are usually disintegrated by shredding and highly elastic polyurethane fibers can block and clump the shredders.[6] Subsequent dissolution and spinning of cellulosic textile fibers are also hampered by trace quantities of elastane.[7] Elastane can be found on the surface or in the core of a yarn, which makes its detection challenging. Recent academic publications and patents in elastane fiber identification have mainly focused on non-invasive methods using traditional NIR spectrometers or hyperspectral cameras.[8–12] Most of these methods did not specifically focus on detecting elastane in cotton or elastane as a minor component but focused on classifying broader textile material categories. Studies including elastane blends as one of the textile categories utilized mainly linear and non-linear discrimination methods.[10,11] Hohmann *et al.* and Langeron *et al.* mentioned poor separability of elastane using traditional point spectrometers and linear class models.[8,9] In addition, Cura *et al.* found that elastane content had a larger influence on the detectability of elastane in cotton fabrics than its location in the fabric.[12]

[a]*VTT Technical Research Centre of Finland Ltd, PO Box 1000 02044 VTT Espoo, Finland. E-mail: ella.mahlamaki@vtt.fi*
[b]*Aalto University, School of Chemical Engineering, Department of Bioproducts and Biosystems, PO Box 16300 00076 Aalto, Finland*

† Electronic supplementary information (ESI) available. See DOI: https://doi.org/10.1039/d5an00107b

Our method offers three distinct aspects of novelty compared with the current alternatives in the fiber identification field. First, we focus on cotton where elastane is used as a minority component and show how fabrics with 2–6% elastane were reliably identified with median true positive and true negative rates of 89–97% based on randomized resampling. Second, we illustrate how outlier fabrics and measurements can be automatically identified and how averaging across individual pixel spectra improved classification accuracy by reducing sampling uncertainty. Outliers are important as fabrics with incorrect labels can distort the chemical subspace described by the class model. In addition, averaging across individual pixel spectra provides a sampling advantage compared to traditional point spectrometers, which determine spectra from a single localized area within a fabric, because both chemical and physical properties are known to influence NIR measurements.[13,14] Third, we used class modelling which offers clear benefits for model training compared with commonly used discriminant classifiers. One-class classifiers enable modelling a new class by training a separate class model to describe the features of that class without representative training objects from the other classes. Overall, we showcase a novel non-invasive alternative to time-consuming chemical methods for elastane identification that can take us a step closer to a circular economy of textiles.

2. Experimental

2.1 Sampling and reference measurements

Pure cotton fabrics and cotton–elastane blends were purchased from the local fabric shop Eurokangas, the import and wholesale shop Tekstiilipalvelu, and the fabric sample provider Finlayson. The collected fabrics had different colors, patterns, and weaving techniques. A total of 201 independent fabric samples were collected and the two classes are summarized in Table 1. All collected fabrics were cut to approximately 10 × 10 cm^2 samples for the imaging measurements. Some selected fabrics were analyzed in detail using an optical microscope (manufacturer: Leica; model: DM750; transmitted light microscope with a camera). The fabrics were manually opened, the yarns were unraveled, and the fibers were identified using a 20× magnification.[15,16]

2.2 Imaging spectroscopy

NIR images were obtained using a Specim SWIR 3 imaging spectrograph with a similar imaging setup to that in our previous work. The instrument worked in a line-scanning mode and recorded light intensity from 384 spatial pixels and 288 spectral variables within the wavelength range 967–2560 nm. The field of view was set to approximately 12 cm with a pixel size of approximately 0.1 mm^2. For more details, see Mahlamäki *et al.*[17] or Mäkelä *et al.*[5,18]

The images were initially determined in raw signal intensity counts and later converted to reflectance values using a two-point linear reflectance transformation. This transformation was based on measurements taken from a reflectance target and dark current readings.[19] The noise at extreme wavelengths was eliminated by excluding variables outside the range 1000–2500 nm. Consequently, the number of spectral variables was reduced to 270.

Table 1 Overview of the collected fabrics

Class	Number of fabric objects	Composition reported in the fabric label	
		Cotton (%)	Elastane (%)
Cotton	100	100	0
Cotton–elastane	101	94–98	2–6

2.3 Exploratory analysis and class modelling

Fabric pixels in the reflectance images were separated from the image backgrounds using principal component analysis (PCA). An average spectrum was determined from each fabric and the object spectra were preprocessed using a second derivative Savitsky–Golay polynomial filter[20,21] with a window length of 11 variables. The preprocessed spectra were mean centered and decomposed with conjoint PCA to visualize variations across both classes.[22] The decomposition was determined according to the general PCA model, eqn (1):

$$\mathbf{X} = \sum_{k=1}^{n} \mathbf{t_k} \mathbf{p_k}^{\mathrm{T}} + \mathbf{E_n} \quad (1)$$

where $\mathbf{X}$ denotes the preprocessed and mean centered average object spectra, $\mathbf{t_k}$ and $\mathbf{p_k}$ the orthogonal score and orthonormal loading vectors, respectively, and $\mathbf{E_n}$ the residual matrix after n principal components (PCs). The loadings of the first principal component were determined as the weights which maximized the variation explained by the corresponding scores, eqn (2):[23]

$$\arg\max_{w=1}(\boldsymbol{t}^{T}\boldsymbol{t}) \quad (2)$$

and the loadings of all subsequent PCs were required to be orthogonal to the previous ones. Outliers in the PC scores were identified based on disjoint PCA and clustering. Scores values were determined separately for both classes and the object scores of the first two PCs were divided into two groups based on their Euclidean distances with k-means clustering. The cluster with a lower number of objects was identified as the outlier group and was assumed to include the false positives of that class. These outlier objects were removed from the final sample set.

A supervised class model was then determined for the cotton–elastane class (Table 1) using soft independent modelling class analogy, SIMCA.[24] The class spectra were first decomposed with PCA and two distance metrics determined to assign a class boundary. These distances were the squared Mahalanobis distance of a score object to the center of the model subspace and the squared Euclidean distance to the model subspace, eqn (3) and (4), respectively:

$$T_i^2 = \mathbf{t_i} \left(\frac{\mathbf{T^T T}}{\mathbf{N} - 1} \right)^{-1} \mathbf{t_i^T} \quad (3)$$

$$Q_{\mathrm{res,\,i}} = \mathbf{e_i}\mathbf{e_i^T}, \quad (4)$$

where $\mathbf{t_i}$ denotes the score vector of an object, $\mathbf{T}$ the score vectors of the training objects, N the number of training objects, and $\mathbf{e_i}$ a vector of model residuals for an object. The two distances were then used to define a combined distance, c, for supervised classification, eqn (5):

$$c = \frac{T^2}{T_{\mathrm{lim}}{}^2} + \frac{Q_{\mathrm{res}}}{Q_{\mathrm{res_{lim}}}} \quad (5)$$

where $T_{\mathrm{lim}}{}^2$ and $Q_{\mathrm{res_{lim}}}$ denote critical distances based on a chosen confidence level. These critical distances were determined according to Jackson using a confidence level of 95%.[25] An object was then considered to belong to the cotton–elastane class if it fulfilled the classification rule, eqn (6):

$$c \leq c_{\mathrm{lim}} \quad (6)$$

where c_{lim} denotes the critical limit value for the combined index alternative discussed by Vitale *et al.*[24]

Training and test sets were generated randomly by selecting one third of the cotton–elastane objects to the test set with all the cotton objects. A suitable number of PCs for the SIMCA classifier was identified through Monte Carlo cross-validation.[26] Two thirds of the training objects were randomly selected to a cross-validation training set and the true positive rate (TPR) of the remaining cross-validation test set objects was determined based on the number of PCs used for class description. This cross-validation procedure was repeated 1000 times and the number of PCs with a median true positive rate closest to the confidence level 95% was selected for the final classifier. Additional resampling was then performed by randomly assigning the objects to training and test sets during 1000 resampling iterations and the distributions of the TPR and true negative rate (TNR) were determined. The analysis workflow is visualized in Fig. 1.

The effect of sampling was evaluated by varying the number of pixels used for calculating the average spectrum of each fabric object. Squared regions of interest of 1–1024 pixels were selected from the center of each image and the median true positive rates were determined with a similar Monte Carlo cross-validation procedure as described above. The analyses were performed using in-house scripts developed in Matlab® (The MathWorks, Inc.) including functions from the PLS toolbox (Eigenvector Research, Inc.).

3. Results and discussion

3.1 Methodological details

We obtained NIR images of cotton fabrics with 0–6% elastane to develop a non-invasive method to reliably detect elastane in cotton. Fig. 2a shows a visualization of the imaging principle. The fabric spectra acquired from the images were determined by averaging over individual pixel spectra (Fig. S1a†) and were preprocessed with Savitzky–Golay filtering (Fig. S1b†). The second order derivation in Savitzky–Golay filtering transformed positive reflectance peaks into negative ones and resulted in inverted peaks in the preprocessed spectra and the following loadings. The preprocessed average spectra of the fabrics were first decomposed with PCA to systematically evaluate the differences in the sample set. The first two principal components explained 82% of the variation in the spectra. Scores of the first two PCs are shown in Fig. 2b. Most of the cotton–elastane class objects showed lower score values on the first principal component than the cotton class. The loadings (Fig. 2b) indicated that these lower score values were associated with negative loadings in preprocessed spectra at approximately 1431 and 1483 nm, which generally correspond to N–H vibrations in NIR spectra.[27,28] The loadings also showed the highest values at 1920 nm, which could be assigned to C=O vibrations in the CONH structure.[27,28] The N–H, O–H and C=O vibrations also showed higher values in the region 2060–2100 nm.[27,28] The positive score values of the cotton class on the first principal component suggested higher values

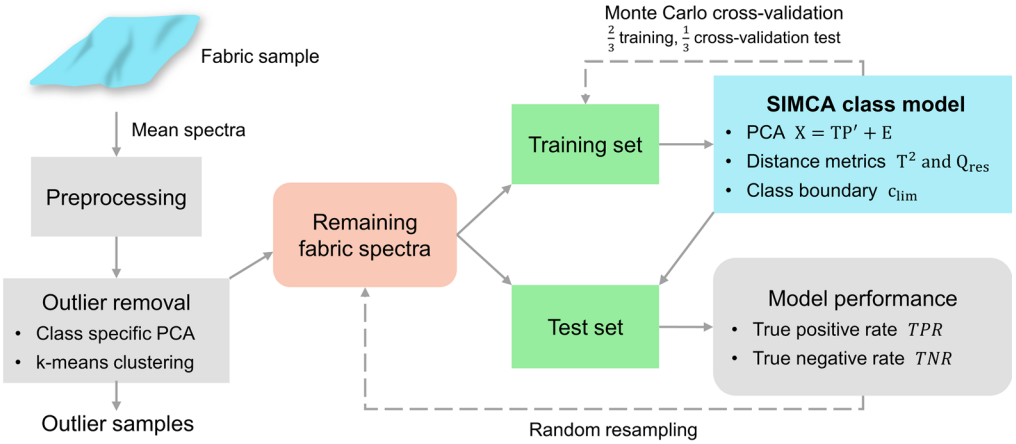

Fig. 1 A image analysis and class modelling flowchart. Principal component analysis (PCA) reduces data dimensionality while preserving variance, and soft independent modelling of class analogy (SIMCA) builds a PCA-based classification model for known groups and assigns new samples based on similarity.

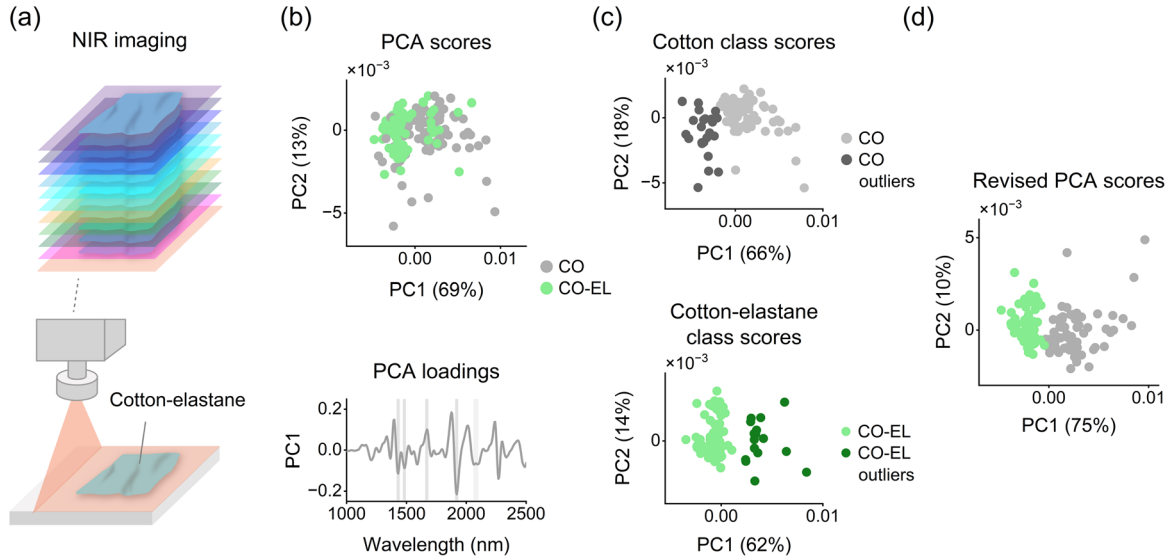

Fig. 2 An illustration of the imaging principle modified from Mahlamäki *et al.*[17] in (a), conjoint principal component (PC) scores across both classes (CO denoting cotton and EL elastane) and respective principal component loadings with the most important wavelength differences in (b), disjoint class specific principal component scores with identified outliers colored in (c), and revised conjoint principal component scores after outlier removal in (d). The wavelengths marked in the loading plot in (b) are discussed in text.

of preprocessed spectra at 1670 nm. We, however, did not find credible assignment for 1670 nm, but it has been previously reported for C–H vibrations in lignin.[29] Overall, interpretation of the PC loadings suggested that the main spectral variations which separated the two classes were mainly associated with the vibrational modes of nitrogen and oxygen structures in elastane. Cotton and cotton–elastane fabrics are visualized on several discussed wavelengths in Fig. S2.†

Scores of the first two PCs, however, showed an overlap in the two fabric classes. Some cotton objects were located over the cotton–elastane class and some cotton–elastane objects were located over the cotton class in the PC score space, see Fig. 2b. This overlap suggested that some of the fabric labels were not in line with the information in the NIR spectra. We decomposed the two classes separately with disjoint PCA and separated the class scores of the first two PCs into two groups with *k*-means clustering to determine the overlapping objects. The results are shown in Fig. 2c. The majority groups in both classes were assumed to be true representatives of that class and the minority groups were deemed as potential outliers. There were altogether 38 potential outliers, 21 in the cotton class and 17 in the cotton–elastane class, which was 19% of our sample set. The disjoint PCA loadings are given in Fig. S3 in the ESI† which shows that the wavelength differences of the majority and minority groups were associated with the same wavelengths as shown in Fig. 2b. These results suggested that some cotton fabrics likely contained synthetic fibers and some cotton–elastane fabrics did not contain elastane, or that the elastane was not visible in the NIR measurements.

We manually unraveled the outlier fabrics and visually inspected the separated fibers with a microscope to confirm our observations on the potential outliers. The results showed that the outlier fabrics with a cotton label did contain synthetic fibers and four of the fabrics also contained elastane. The microscopic structural images of these findings are shown in Fig. S4.† Synthetic fibers and elastane were also found in most of the cotton–elastane outliers (Fig. S5†). According to European Union Regulation no. 1007/2011 fabrics are allowed to have up to 2% of extraneous fibers without mentioning it on the fabric label if they are added unintentionally during production.[30] This regulation accounts for small changes in fiber content during a manufacturing process. The NIR measurements were influenced not just by the extraneous fibers, but also by the structure of the fabrics. Five of the cotton–elastane outliers had a knitted fabric structure, where elastane was in the core of the fiber surrounded by cotton yarn (Fig. S6†).[31–33] This suggested that NIR light had not penetrated through the cotton yarn to detect the elastane fibers. Eleven of the outliers had a woven structure, where elastane yarn was found only in the weft direction, and one fabric contained synthetic fibers other than elastane. Moussa *et al.* (2006) studied the effects of the fabric structure on light scattering from fibers and found that the highest back-scattering occured when the direction of incident light was perpendicular to the incidence plane for yarn samples and to the weft direction in the woven fabric.[34] In addition to the direction of the light, the penetration depth of NIR light into the sample must be sufficient to detect elastane fiber in the core of the yarn. The fabric structures of the potential outliers containing elastane suggested that elastane was not on the surface of the fabric or elastane fiber, in relation to the incidence plane, was in the direction of increased scattering, and was not visible in the NIR spectra. All potential outlier fabrics in the minority groups were deemed as outliers and removed from the final sample set. After outlier removal the conjoint PC scores showed two clusters, and the loadings showed that the wave-

length differences of the cotton and cotton–elastane groups were associated with the same wavelengths as shown in Fig. 2b. The revised PC scores are shown in Fig. 2d. Overall, disjoint PCA and clustering provided a convenient way to automatically identify fabrics or NIR measurements which were not in line with the information reported in the fabric label.

We focused on training a SIMCA classifier specifically for the cotton–elastane class and divided the objects of that class into training and test sets. All cotton class spectra were designated to the test set. Significant features in the training set were extracted with a PCA model, which was used to determine the relevant model distances for the classifier. An illustration of the model distances and the class boundary in a one-dimensional principal component model is shown in Fig. 3a. An appropriate number of PCs was estimated by Monte Carlo cross-validation.[26] The results showed that a median true positive rate closest to the predetermined 95% confidence level was achieved with only one PC based on 1000 random sampling iterations, see Fig. 3b. Cross-validation performance started to decrease with more than one PC, which indicated that a one component class model was sufficient to reliably describe the properties of the target class.

We also determined cross-validation performance with different preprocessing combinations based on first and second derivative Savitzky–Golay filtering and standard normal variate transformation.[35] The results are shown in Fig. S7,† where we report the effect of derivative filtering on different filter window lengths. A wider filter window led to excessive smoothing and removed important features in the average spectra, while a narrower filter window likely generated excess noise to the signals. An appropriate processing method was important to enhance the chemical features of elastane. We evaluated the effect of pixel averaging by controlling the number of pixels used for determining the average fabric spectra. As shown in Fig. 3c, median true positive rates were closest to the predetermined confidence level 95% using 1024 or all fabric pixels. Cross-validation performance decreased with a decrease in the number of pixels used for averaging. Using fewer pixels for averaging increased sampling uncertainty and reduced our capability to extract chemically relevant features from the spectra.

We then determined the performance of the final SIMCA classifier with the randomly chosen test set. Classification of the test set spectra resulted in a true positive rate of 93% and a true negative rate of 97% with an overall accuracy of 96%. Fig. 3d shows the squared Mahalanobis distances within the model and the squared Euclidean distances to the model for the test set objects with the derived class boundary, and Fig. 3e reports the confusion matrix based on the test set. In Fig. 3d the axes are logarithmically transformed for visualization, which makes the linear class boundary appear non-linear. Two cotton–elastane fabrics and two cotton fabrics were misclassified. The misclassified fabrics were similarly manually unraveled as the outliers. The microscopy images of the two misclassified cotton fabrics showed synthetic fibers (Fig. S8†). The misclassified cotton–elastane fabrics contained 3% of elastane based on the fabric label. The elastane fiber was found in the core of the fibers from both misclassified fabrics, which suggested that elastane in these fabrics was not visible in the NIR measurements.

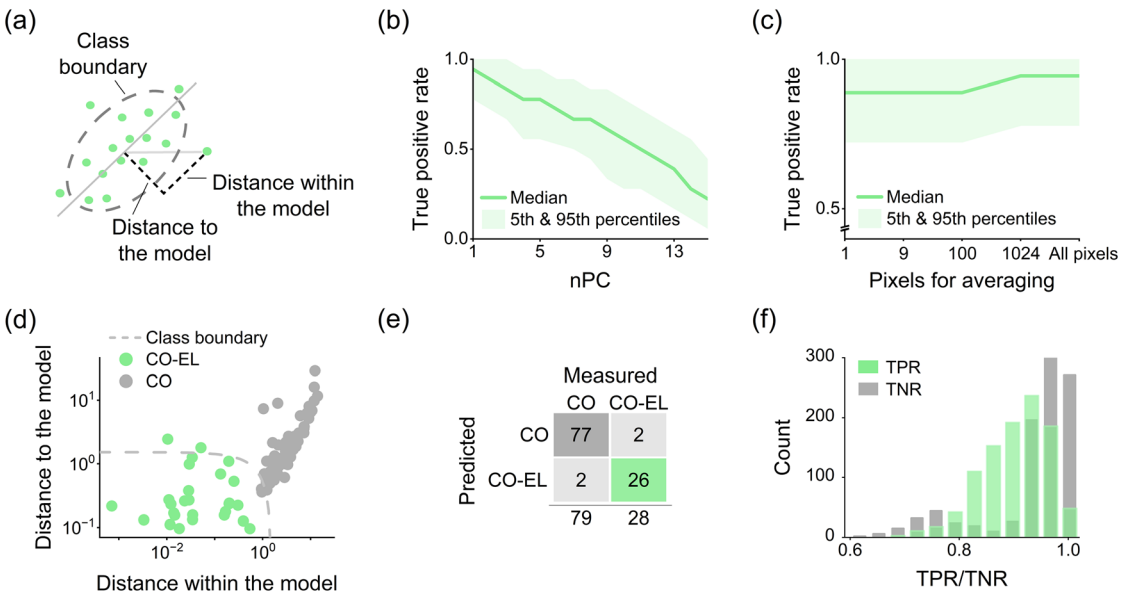

Fig. 3 An illustration of the distance metrics and the class boundary for a one-dimensional SIMCA model in (a), the median true positive rates (TPR) of the first 15 principal components (PC) during cross-validation with the respective 5th and 95th percentiles in (b), the cross-validation median TPRs for varying number of pixels used to determine average fabric spectra and the respective 5th and 95th percentiles in (c), test set classification results of the SIMCA model trained for cotton–elastane (CO-EL) fabrics in (d) with the respective confusion matrix in (e). The axes in (d) were logarithmically transformed for visualization, which makes the linear class boundary appear non-linear. TPR and true negative rates (TNR) of the SIMCA model based on random resampling (f).

As shown in Fig. 3d and e, we tested the SIMCA classifier after we had randomly assigned one third of the cotton–elastane spectral objects in the remaining sample set to a separate test set with the cotton objects. There were thus 56 objects in the training set and 107 objects in the corresponding test set (Fig. 3e). The results suggested promising classifier performance based on determined TPR and TNR which, however, varied depending on which exact objects were assigned to the training and test sets. To account for this variation, we performed additional resampling by randomly assigning the objects to training and test sets during 1000 resampling iterations and determined distributions of TPR and TNR. The results are illustrated in Fig. 3f. The randomized resampling iterations led to median true positive and true negative rates of 89% and 97%, which indicated that our classifier correctly identified cotton fabrics with small amounts of elastane independent of how the training and test set objects were chosen.

3.2 Practical relevance

Elastane accounts for 1% of the global textile fiber production as only a small share is needed to provide elasticity and additional wear comfort in textiles. Fabrics made from natural fibers such as cotton or wool often contain 1–5 wt% elastane and polyester or polyamide fabrics may contain up to 20 wt%.[36] These natural and synthetic fibers most often blended with elastane account for approximately 87% of global fiber production,[3] but data on the share of fabrics containing elastane are not available. The share of elastane containing textiles has increased drastically in the past decade due to increased elastane production, with no indication that the use of elastane will decrease soon. Elastane detection is important for textile recycling as elastane fibers can block and clump defiberization and shredding equipment during recycling. Mechanical recycling of fibers containing elastane results in lower quality yarns and residual amounts of polyurethane impede chemical recycling of polyester and cellulosic fibers.[7,36] Methods to identify and isolate elastane-containing textile waste are therefore key to ensure efficient recycling of polyester, polyamide, and cellulosic fibers.

NIR imaging spectroscopy provides an appealing alternative for fast and non-invasive identification of elastane in textiles. Imaging spectrometers determine material-specific chemical fingerprints from every pixel of an image scene, which provides large amounts of data. These data can then be used for training image classification or regression models as part of high-throughput and automated sorting systems, which are currently breaking ground in the textile field.[37] However, scaling imaging spectrometers for industrial applications presents challenges such as increased costs, demands on processing speed and complexity. Instruments working on wider NIR wavelength regions, such as 1000–2500 nm, generally use expensive cryogenically cooled MCT detectors, whereas imaging in shorter regions up to 1700 nm can be performed with cheaper InGaAs sensors.[38,39] The required wavelength region is determined by the application and the spectral features as different chemical bonds interact with light on specific wavelengths. The speed of the measurement is specified by spectral and spatial resolutions, the frame rate of the detector, and the speed of the conveyor belt. These determine how many pixels are imaged and how quickly they are captured, which then defines the time required to process the data.

Beyond costs and speed, a significant challenge for industrial applications is the large amount of variation and contaminants in post-consumer textile materials.[12] Variations in fabric types, sources, quality and condition generate a lot of spectral variation. Contaminants, such as dirt, oil, or residues from previous processing steps, can change the spectral signature of the fabric as they may introduce additional absorption or reflection features that are not representative of the target fabric material. Detecting detailed properties or minor fiber components in fabrics, such as elastane, thus requires that the collected textile waste is first sorted.[37]

Here, we have focused on a small problematic category of textile waste and presented on lab-scale how 2–6% elastane can be detected in cotton fabrics, but future efforts should acknowledge these challenges when developing machine vision algorithms for industrial applications of textile material identification. Based on the principles of our classification model, we believe that our method is applicable also to fabrics with elastane content outside the range 2–6%, and generalizable to other elastane fabrics with similar characteristics as long as the classifier can be trained on correct labels and the elastic fiber is visible in the NIR spectra.

Conclusions

We have shown how 2–6% elastane was identified in consumer cotton fabrics using NIR imaging spectroscopy and class modelling. Our spectral image classifier showed median test set true positive and true negative rates of 89–97% based on randomized resampling and indicated that the relevant spectral features were associated with the vibrational modes of nitrogen and oxygen structures in elastane. We also showed how outlier samples and measurements could be automatically identified and how averaging across individual pixel spectra improved classification accuracy by reducing sampling uncertainty. Our class modelling approach would in the future enable training new class models with only a set of target samples without representative training objects from all the other classes. These results are significant as they indicate a novel non-invasive alternative to time-consuming chemical analyses for elastane identification. In the future, this will enable guiding the right materials to the appropriate recycling paths bringing us a step closer to a circular economy of textiles.

Author contributions

I. S-.H. and M. M. conceptualized the study, acquired the study resources, and administered the project. M. M. contributed to acquiring the funding. E. M., I. S-.H. and M. M. devised the methodology, and performed the investigation with T. K. E. M. and M. M. developed the software for formal ana-

lysis of the data, validated the results and performed the visualization. E. M. carried out the formal analysis and curated the data. E. M. and M. H. wrote the original draft, and revised and edited the draft with I. S-.H. and M. M. M. H. and M. M. supervised the study.

Data availability

The dataset and codes used in this work have not been made available due to our pending patent application.

Conflicts of interest

The authors declare the following financial interests/personal relationships which may be considered as potential competing interests: VTT Technical Research Centre of Finland Ltd and Aalto University have submitted a patent application (PC23066FI) related to this work.

Acknowledgements

This work was financially supported by the Strategic Research Council established within the Research Council of Finland under grant agreement no. 352698 and by the Research Council of Finland Flagship Programme: Finnish Center for Artificial Intelligence FCAI.

References

1 O. Bayer, W. Siefken, H. Rinke, L. Orthner and H. A. Schild, *Ger. Pat*, DE 728981, 1937.
2 D. Veit, *Fibers: History, Production, Properties, Market*, Springer International Publishing, 2023.
3 Textile Exchange, Preferred Fiber & Materials Market Report Foreword, 2022.
4 The Fiber Year 2023 – World Survey on Textiles & Nonwovens, 2023.
5 M. Mäkelä, M. Rissanen and H. Sixta, *Analyst*, 2021, **146**, 7503–7509.
6 E. Boschmeier, V.-M. Archodoulaki, A. Schwaighofer, B. Lendl, W. Ipsmiller and A. Bartl, *Resour., Conserv. Recycl.*, 2023, **198**, 107215.
7 L. Villar, I. Schlapp-Hackl, P. B. Sánchez and M. Hummel, *Biomacromolecules*, 2024, **3**, 1942–1949.
8 M. Hohmann, C. Krick Calderon and P. Neumaier, WO 2020/109170 A1, 2018.
9 Y. Langeron, M. Doussot, D. J. Hewson and J. Duchêne, *Eng. Appl. Artif. Intell.*, 2007, **20**, 415–427.
10 F. Vandeputte, M. Vandeputte and P. Vandeputte, US 2022/0214273 A1, 2022.
11 T. Gupta, S. Bajaj and M. Wang, WO 2023/069913 A1, 2022.
12 K. Cura, N. Rintala, T. Kamppuri, E. Saarimäki and P. Heikkilä, *Recycling*, 2021, **6**, 1–12.
13 D. Quintero Balbás, G. Lanterna, C. Cirrincione, R. Fontana and J. Striova, *Eur. Phys. J. Plus*, 2022, **137**, 85.
14 E. Cleve, E. Bach and E. Schollmeyer, *Anal. Chim. Acta*, 2000, **420**, 163–167.
15 J. Hu, B. Kumar and J. Lu, *Handbook of Fibrous Materials*, Wiley, 2020.
16 R. R. Mather, R. H. Wardman and S. Rana, *The Chemistry of Textile Fibres*, Royal Society of Chemistry, 3rd edn, 2023.
17 E. Mahlamäki, I. Schlapp-Hackl, M. Rissanen, M. Hummel and M. Mäkelä, *Resour., Conserv. Recycl.*, 2023, **193**, 106984.
18 M. Mäkelä, M. Rissanen and H. Sixta, *Resour., Conserv. Recycl.*, 2020, **161**, 105007.
19 J. Burger and P. Geladi, *J. Chemom.*, 2005, **19**, 355–363.
20 J. Burger and P. Geladi, *J. Near Infrared Spectrosc.*, 2007, **15**, 29–37.
21 R. J. Barnes, M. S. Dhanoa and S. J. Lister, *Appl. Spectrosc.*, 1989, **43**, 772–777.
22 R. G. Brereton, *J. Chemom.*, 2011, **25**, 225–246.
23 R. Bro and A. K. Smilde, *Anal. Methods*, 2014, **6**, 2812–2831.
24 R. Vitale, M. Cocchi, A. Biancolillo, C. Ruckebusch and F. Marini, *Anal. Chim. Acta*, 2023, **1270**, 341304.
25 J. E. Jackson, *A Use's Guide to Principal Components*, Wiley, 1991.
26 Q.-S. Xu and Y.-Z. Liang, *Chemom. Intell. Lab. Syst.*, 2000, **56**, 1–11.
27 B. G. Osborne, T. Fearn and P. H. Hindle, *Practical NIR spectroscopy with applications in food and beverage analysis*, Wiley, 2nd edn, 1993.
28 P. Williams, J. Antoniszyn and M. Manley, *Near Infrared Technology: Getting the best out of light*, African Sun Media, 1st edn, 2019.
29 M. Schwanninger, J. C. Rodrigues and K. Fackler, *J. Near Infrared Spectrosc.*, 2011, **19**, 287–308.
30 Regulation (EU) No 1007/2011 of the European Parliament and of the Council of 27 September, *Official Journal of the European Union*, 2011.
31 N. T. Akankwasa, M. Q. Siddiqui, E. Kamalha and L. Ndlovu, *Res. Rev. Polym.*, 2013, **4**, 127–137.
32 A. B. Dhouib, S. El-Ghezal and M. Cheikhrouhou, *J. Text. Inst.*, 2006, **97**, 167–172.
33 O. Babaarslan, *Text. Res. J.*, 2001, **71**, 367–371.
34 A. Moussa, D. Dupont, D. Steen, X. Zeng and M. Elias, *Color Res. Appl.*, 2006, **31**, 122–132.
35 J.-L. Xu, C. Riccioli, A. Herrero-Langreo and A. Gowen, *J. Spectr. Imaging.*, 2020, **9**, a19.
36 E. Boschmeier, V. M. Archodoulaki, A. Schwaighofer, B. Lendl and A. Bartl, *Polym. Test.*, 2023, **118**, 107920.
37 O. Sahimaa, E. M. Miller, M. Halme, K. Niinimäki, H. Tanner, M. Mäkelä, M. Rissanen, A. Härri and M. Hummel, *Nat. Rev. Earth Environ.*, 2023, **4**, 137–138.
38 Specim, SWIR Technical Datasheet. Available for download at: **https://www.specim.com/products/swir/** (assessed January 17, 2025).
39 Specim, FX17 Technical Datasheet. Available for download at: **https://www.specim.com/products/specim-fx17/** (assessed January 17, 2025).